Development of a Digital Twin to Support the Calibration of a Highly Efficient Spark Ignition Engine

2023-01-1215 Published 26 Jun 2023

Development of a Digital Twin to Support the Calibration of a Highly Efficient Spark Ignition Engine

Toni Tahtouh and Mathieu Andre IFP Energies nouvelles

Federico Millo, Luciano Rolando, and Giuseppe Castellano Politecnico di Torino

Francesco Bocchieri FEV Italia s.r.l.

Luca Cambriglia and Danilo Raimondo POWERTECH Engineering S.r.l.

Citation: Tahtouh, T., Andre, M., Millo, F., Rolando, L. et al., "Development of a Digital Twin to Support the Calibration of a Highly Efficient Spark Ignition Engine," SAE Technical Paper 2023-01-1215, 2023, doi:10.4271/2023-01-1215.

Received: 07 Mar 2023 Revised: 28 Mar 2023 Accepted: 28 Mar 2023

Abstract

The role of numerical simulations in the development of innovative and sustainable powertrains is constantly growing thanks to their capabilities to significantly reduce the calibration efforts and to point out potential synergies among different technologies. In such a framework, this paper describes the development of a fully physical 1D-CFD engine model to support the calibration of the highly efficient spark ignition engine of the PHOENICE (PHev towards zerO EmissioNs & ultimate ICE efficiency) EU H2020 project. The availability of a reliable simulation platform is essential to effectively exploit the combination of the several features introduced to achieve the project target of 47% peak gross indicated efficiency, such as Swumble™ in-cylinder charge motion, Miller cycle combined with high Compression Ratio (CR), lean mixture exploiting cooled low pressure Exhaust Gas Recirculation (EGR) and electrified turbocharging. Particular attention was paid to the definition of a combustion model capable of predicting engine burn rates in highly diluted conditions as well as the likelihood of abnormal combustion phenomena such as knock. A set of preliminary experimental measurements carried out on the first engine prototype was used to assess the reliability of the developed digital twin. Afterwards, the 1D-CFD model was used to identify, under steady state conditions, the optimal setting of calibration parameters in terms of intake valves actuation, throughout the whole engine operating map. Findings demonstrated that the lean and diluted combustion process combined with the high CR of 13.6 and aggressive EIVC strategy enabling unthrottled operation made it possible to achieve the target of 47% peak gross indicated efficiency at part load. When operating at full load, the use of cooled low pressure EGR significantly reduced knock likelihood and permitted to avoid any mixture enrichment, allowing for the achievement of performance targets without incurring in fuel consumption penalties.

Introduction

Despite the legislative targets set by the European Commission of a full electrification of new light-duty vehicles introduced on the EU market by 2035 [1], the development of high-efficiency and environmentally friendly Internal Combustion Engines (ICEs) is still crucial to be on track toward the complete decarbonization of on road-mobility of the future. As a matter of fact, as clearly shown in [2], "*a mix of carbon neutral pathways (energy forms and powertrains) can significantly speed up the transition to Greenhouse Gases (GHG) neutrality compared to single technology scenarios*".

In such a framework, the PHOENICE (PHev towards zerO EmissioNs & ultimate ICE efficiency) EU funded project [3] aims at developing a C SUV-class plug-in hybrid vehicle demonstrator capable to achieve a 10% fuel consumption reduction on a Charge Sustaining (CS) WLTC test with respect to the "baseline" EU6 vehicle currently available on the market, while being fully compliant with the recently announced new EU7 pollutant emissions limits [4], as summarized in Table 1 and Table 2, respectively.

In order to achieve such ambitious targets, requiring a 47% peak gross engine indicated efficiency, the availability of

TABLE 1 Vehicle and Engine Efficiency Targets.

Fuel Consumption	-10% vs Baseline Vehicle (CS WLTC Test)
ICE Efficiency	47% Peak Gross Indicated Eff.

TABLE 2 Pollutants Emissions Targets (RDE).

CO	400 mg/km	CH_4	10 mg/km
NMOG	25 mg/km	HCOH	5 mg/km
NO_x	20 mg/km	N_2O	10 mg/km
PM	2 mg/km	NH_3	10 mg/km
PN (>10nm)	5×10^{10} #/km		

a reliable simulation platform is essential to effectively exploit the synergies between the several technologies that were introduced in the project, such as the Swumble™ high turbulence in-cylinder charge motion to support the use of lean and Exhaust Gas Recirculation (EGR) diluted mixtures at part load, coupled with a high Compression Ratio (CR) and a MultiAir Constantly Variable Valve Lift (CVVL) system, allowing Early Intake Valve Closing (EIVC) strategies to enable unthrottled operation at part load as well as aggressive Millerization of the engine cycle to reduce the knock likelihood at high load.

In this context, this paper describes the development of a fully physical (One-Dimensional Computational Fluid Dynamics) 1D-CFD engine model to support the calibration of the PHOENICE engine. After assessing the reliability of the developed digital twin on a set of preliminary experimental measurements carried out on the first engine prototype, the 1D-CFD model was then used to identify, under steady state conditions, the optimal setting of calibration parameters in terms of intake valves actuation, throughout the whole engine operating map.

Findings demonstrated that the optimal EIVC strategies, identified by means of the numerical simulations, enabling unthrottled operation at part load, in combination with the lean and diluted combustion process and the high CR of 13.6, made it possible to achieve the project target of 47% gross indicated efficiency at part load. On the other hand, when operating at high and full load, the aggressive cycle Millerization and the use of cooled low pressure EGR significantly reduced knock likelihood and permitted to avoid any mixture enrichment, allowing for the achievement of performance targets without incurring in fuel consumption penalties.

The PHOENICE Engine Concept

This activity focused on a new engine concept based on a state-of-the-art 4-cylinder 1.3L turbocharged Direct Injection Spark Ignition (DISI) engine [5]. The former inherits from the latter an all-aluminum engine structure featuring a high stroke to bore ratio, a compact 4-valve combustion chamber with high pressure side fuel injectors, a MultiAir CVVL system [6] and a cylinder head with integrated exhaust manifold. As part of the PHOENICE project, the baseline engine hardware has been upgraded with several novel technologies, illustrated in Figure 1, with the goal of minimizing fuel consumption and pollutant emissions across the entire engine map, while also taking advantage of the potentialities offered by powertrain hybridization.

FIGURE 1 PHOENICE engine features.

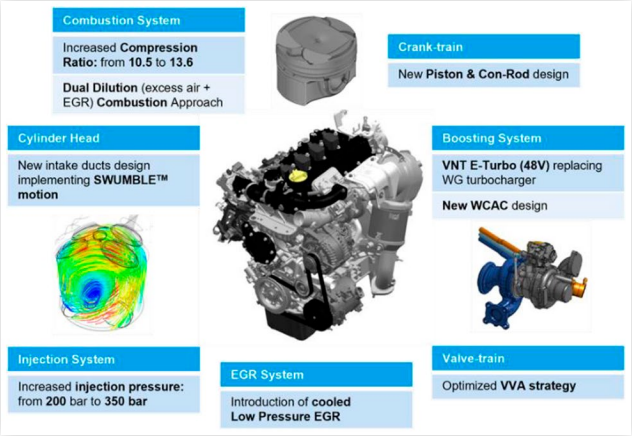

Table 3 summarizes the main PHOENICE engine specifications.

To enhance the fuel conversion efficiency, the combustion chamber has been redesigned to increase the CR up to 13.6 and to enable lean burn operation through a Dual Dilution Combustion Approach (DDCA). This advanced combustion strategy achieves lower combustion temperatures by utilizing both excess air and cooled low pressure EGR. Lower combustion temperatures can reduce cooling losses and energy losses at the exhaust, as well as enable better phased combustion at high loads due to the decreased knock likelihood. It also results in reduced pumping losses during the gas exchange process at low loads [7, 8, 9]. In particular, EGR offers additional benefits on knock mitigation, a critical aspect because of the high CR, improving mixture characteristics in terms of heat capacity and polytrophic exponent [10]. To support the ultra-lean combustion approach, the fuel injection system has been upgraded to reach injection pressures up to 350 bar. Furthermore, the geometries of intake ducts and ports have been optimized to implement the Swumble™. This recently developed charge motion concept combines swirl and tumble motions to consistently increase in-cylinder turbulence intensity, with beneficial effects on flame propagation velocity [11, 12, 13, 14]. On the turbocharging side, a 48V electrified system embedding a Variable Nozzle Turbine (VNT) replaced the

TABLE 3 PHOENICE engine specifications.

Specification	Value
N. of Cylinders	4 in-line
Displacement	1332 cm^3
Bore x Stroke	Ø 70 mm x 86.5 mm
Stroke/Bore	1.24
Compression Ratio	13.6:1
Number of Valves	16
VVA System	MultiAir II (intake only)
Fuel Injection System	GDI
Turbocharging	VNT E-Turbo
Fuel	E10 gasoline (RON 97.3)
Rated Power (target)	100 kW @ 4500 RPM
Rated Torque (target)	218 Nm @ 3500 RPM

baseline Wastegate (WG) turbocharger to ensure the necessary boost pressure in all operating conditions. Additionally, the E-Turbo can recover waste enthalpy from exhaust gases and reduce turbo-lag phenomena during transient maneuvers [15]. Finally, the fully variable MultiAir valve actuation system enables Miller cycle exploitation through Early Intake Valve Closing (EIVC) or Late Intake Valve Closing (LIVC) load control. Both these strategies have proven to minimize pumping losses at part load thanks to unthrottled operation and to promote knock mitigation at high load thanks to a reduction in the effective CR [16, 17, 18].

Numerical Model Description and Validation

Model Description

A digital twin of the PHOENICE engine was developed in the commercially available software GT-Suite, a 1D-CFD code developed by Gamma Technologies [19]. This virtual test rig features a predictive combustion model, the SITurb [20, 21, 22], through which it is possible to achieve a reliable estimation of the burn rate over a wide range of Air-to-Fuel Ratios (AFRs), EGR rates and valve timings. In particular, the combustion process of a spark-ignited engine, that is characterized by a turbulent propagating flame, is simulated through a two-zone approach in which the combustion chamber is subdivided into burned and unburned gas regions. The turbulent flame brush is modelled via a spherical propagation and with a typical entrainment and burn-up approach, where the flame wrinkling effect is captured by the turbulent flame speed [22]. More in details, the entrained mass (M_e) rate of the unburned air-fuel mixture in the flame front is dependent on the flame area (A_f), the unburned gas density (ρ_u), and the sum of the turbulent and laminar flame speeds (S_T and S_L, respectively), as expressed by Equation 1:

$$\frac{dM_e}{dt} = \rho_u \cdot A_f \cdot \left(S_T + S_L\right) \tag{1}$$

S_T is calculated through Equation 2, where R_f, u' and L_t refer to flame radius, turbulent intensity and turbulent length scale, respectively.

$$S_T = \mathbf{C_S} \cdot u' \cdot \left(1 - \frac{1}{1 + \frac{\mathbf{C_k} \cdot R_f^2}{L_t^2}}\right) \tag{2}$$

In Equation 2, two calibration parameters are present: the turbulent flame speed multiplier (C_S), which globally scales the turbulent flame speed, and the flame kernel growth multiplier (C_k), which scales the flame front evolution. A further calibration parameter, the dilution effect multiplier (C_D), is instead adopted to tune the effect of diluents such as exhaust residuals and EGR on the laminar flame speed, which is calculated by Equation 3:

$$S_L = \left(B_m + B_\phi \cdot \left(\phi - \phi_m\right)^2\right) \cdot \left(\frac{T_u}{T_0}\right)^\alpha \cdot \left(\frac{p}{p_0}\right)^\beta \cdot \ldots \cdot \left(1 - 0.75 \cdot \mathbf{C_D} \cdot \left(1 - \left(1 - 0.75 \cdot \mathbf{C_D} \cdot \left[D_i\right]\right)^7\right)\right) \tag{3}$$

where ϕ is the in-cylinder equivalence ratio, T_u is the temperature of the unburned gas, p is the in-cylinder pressure and D_i is the mass fraction of the diluents in the unburned zone. B_m, B_ϕ, ϕ_m, T_0, p_0, α and β are model constants. Finally, Equation 4 is used to determine the burn rate of the entrained unburned mass M_u:

$$\frac{dM_b}{dt} = \frac{M_u}{\tau} = \frac{M_e - M_b}{\tau} \tag{4}$$

where τ is assumed to be the time needed by the laminar flame speed to cover the Taylor microscale (λ) of turbulence, expressed by Equation 5. Here, C_λ, the Taylor length scale multiplier, is a further calibration parameter inversely proportional to the burn-up rate.

$$\tau = \frac{\lambda \cdot \mathbf{C_\lambda}}{S_L} \tag{5}$$

A critical aspect of the virtual test rig is the knock prediction. Indeed, the increased compression ratio and boosting levels may lead to a higher knock likelihood. As a result, a knock model based on the approach proposed by Livengood and Wu [23] was used in this study. It states that the auto-ignition of the end gas occurs when:

$$\int_{t=0}^{t_{knock}} \frac{1}{\tau} dt = 1 \tag{6}$$

where τ is the induction time of the air-fuel mixture and t_{knock} is the time corresponding to the auto-ignition instant (computed from the start of compression). Among the empirical relationships for induction time calculation available in the scientific literature [24, 25, 26], the so-called Kinetics-Fit model, proposed by Gamma Technologies [19], was preferred for this work since it considers the dependence of the induction time from the mixture composition in terms of diluents (e.g., EGR) and it can reproduce the Negative Temperature Coefficient (NTC) behavior [27, 28] according to Equation 7. This model features two calibration parameters, i.e., the Knock Induction Time Multiplier (KITM) and the Activation Energy Multiplier (AEM):

$$\tau = \boldsymbol{KITM} \cdot a_i \cdot \left(\frac{RON}{100}\right)^{b_i} \cdot \left[Fuel\right]^{c_i} \cdot \left[O_2\right]^{d_i} \cdot \left[D_i\right]^{e_i} \cdot \ldots \cdot \exp\left(\frac{f_i}{\boldsymbol{AEM} \cdot T_u}\right) \tag{7}$$

where RON is the fuel Research Octane Number, [Fuel] and [O_2] are respectively fuel and oxygen concentrations in [mol/m^3], T_u is the unburned gas temperature, [D_i] is the sum of N_2, CO_2, and H_2O concentrations in [mol/m^3] while quantities from a_i to f_i are model constants.

Model Validation

The four tuning parameters of the SITurb model (i.e., C_S, C_k, C_D and C_λ) and the two tuning parameters of the knock model, (i.e., KITM and AEM) were calibrated using a preliminary set of 48 experimental data (see Figure 2) collected on a first PHOENICE engine prototype that still retained the baseline engine turbocharger and exhaust line. These 48 points were defined to cover most of the operating map, while reaching only a limited high load (corresponding to the red points in Figure 2) to preserve the integrity of the first prototype. The engine was run under stoichiometric conditions (lambda = 1), without EGR, and with a Knock-Limited Spark Advance (KLSA). Afterwards, the model was validated on three engine operating points (marked with a yellow star in Figure 2), corresponding to a low, medium, and high load, respectively.

The same methodology previously discussed in [20, 21] was applied for the identification of the four tuning parameters of the SITurb model. It relies on a Design of Experiment (DoE) strategy combined with a Genetic Algorithm (GA) optimum search [19] and it aims at minimizing the error between the experimental and predicted burn rates. The GA requires the definition of the number of generations and the related population size. The population is composed of individuals, which are vectors representing a combination of calibration parameters. The product of the number of generations and the population size yields the total number of designs. The optimization starts with the random selection of the values for the individuals of the population of the first generation. The values are taken inside the range specified by the user. After simulating the entire first generation, the user-defined objective function — the burn rate error for this application — is used to assess the fitness of each individual. The population is then evolved for the following generation using the individuals which result in the lowest burn rate error. At the end of the optimization process, the GA provides the optimal individual, i.e., the vector representing the combination of optimal calibration parameters, leading to the minimum burn rate error.

FIGURE 2 Set of experimental test points performed on the engine prototype.

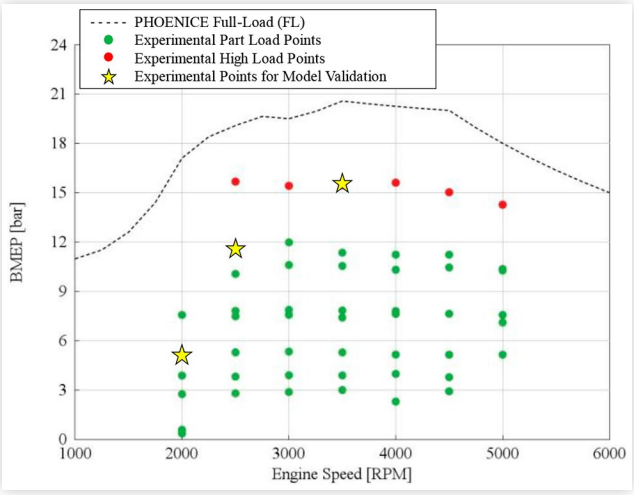

© Authors

The optimized values of the calibration parameters of the SITurb combustion model are reported in Table 4.

Afterwards, the two calibration parameters of the knock model, i.e., KITM and AEM, were adjusted to obtain an induction time integral equal to one with the imposed experimental knock limited spark advance. This tuning was performed on the high load points identified by the red dots in Figure 2.

Once the optimal SITurb and knock model parameters had been defined, the complete engine model was benchmarked against the experimental data to assess its accuracy and reliability. The values of Indicated Mean Effective Pressure (IMEP), Pumping Mean Effective Pressure (PMEP), Volumetric Efficiency (referred to the air conditions in the intake manifold) and in-cylinder peak pressure, depicted in Figure 3, highlight a satisfactory agreement with a maximum error just over 5%. Only the correlation plot of the in-cylinder peak pressure appears to be slightly more scattered.

Finally, the three different operating conditions marked with a yellow star in Figure 2 served as validation test for the engine model. As reported in Figure 4, the simulated pressure and burn rate profiles are closely aligned with experimental traces.

TABLE 4 Optimized parameters of the SITurb model.

Calibration Parameter	Value
C_S	1.05
C_k	2.66
C_D	0.45
C_λ	1.82

© Authors

FIGURE 3 Correlation plots for the selected operating conditions. (a): IMEP – (b): PMEP – (c): In-cylinder peak pressure – (d): Volumetric Efficiency.

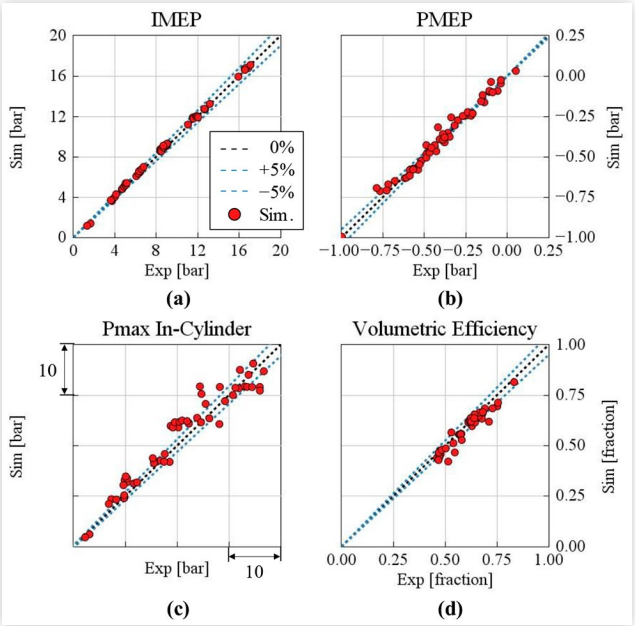

© Authors

FIGURE 4 Comparison of measured and simulated Pressure Traces and Burn Rates. (a): 2000 RPM x 5.15 bar BMEP – (b): 2500 RPM x 11.55 bar BMEP – (c): 3000 RPM x 15.43 bar BMEP.

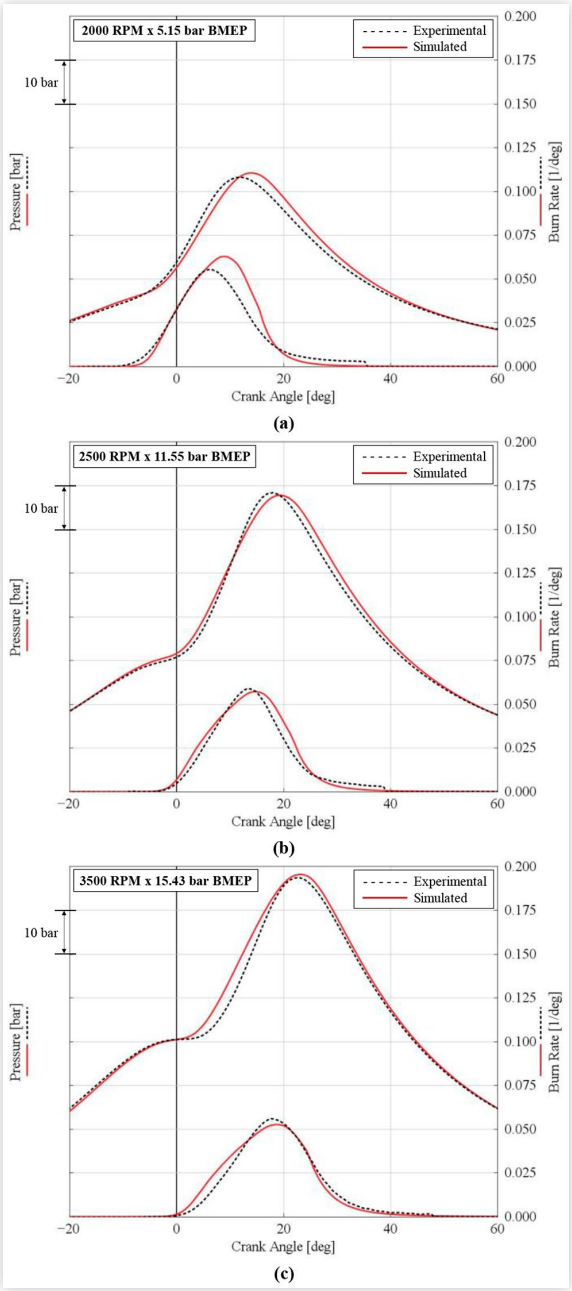

Engine Steady-State Virtual Calibration

Virtual Calibration Set-Up

After the above-described correlation against the first set of experimental data measured under stoichiometric operation without EGR, the developed 1D-CFD engine model was used as a virtual test rig to perform a preliminary calibration for the entire engine map. The aim of this activity was to assess the potential in terms of fuel consumption benefits of the novel hardware technologies implemented to enable the DDCA concept, and to support the successive calibration at the engine test bench. First, the model was upgraded to include the new E-Turbo specifications and the revised Exhaust After-Treatment System (EATS) components. The E-Turbo enhanced turbine inlet temperature was considered when updating the turbocharger controls. It was then important to re-optimize the gas exchange process to account for the backpressure increase produced by the modified exhaust line, which has a detrimental impact on the pumping work. Finally, the previously calibrated knock model was exploited to detect knocking conditions and adjust the spark timing accordingly to run the engine with a KLSA.

The virtual calibration was performed providing to the model the lambda and EGR maps shown in Figure 5, which were extrapolated from a preliminary test campaign conducted on a Single Cylinder Engine (SCE) prototype. The purpose was to evaluate the DDCA potentialities at the very early stages of the project through an initial investigation on the optimal combination of lambda and low pressure cooled EGR to maximize fuel conversion efficiency.

FIGURE 5 Engine maps for virtual calibration. (a): Lambda – (b): EGR.

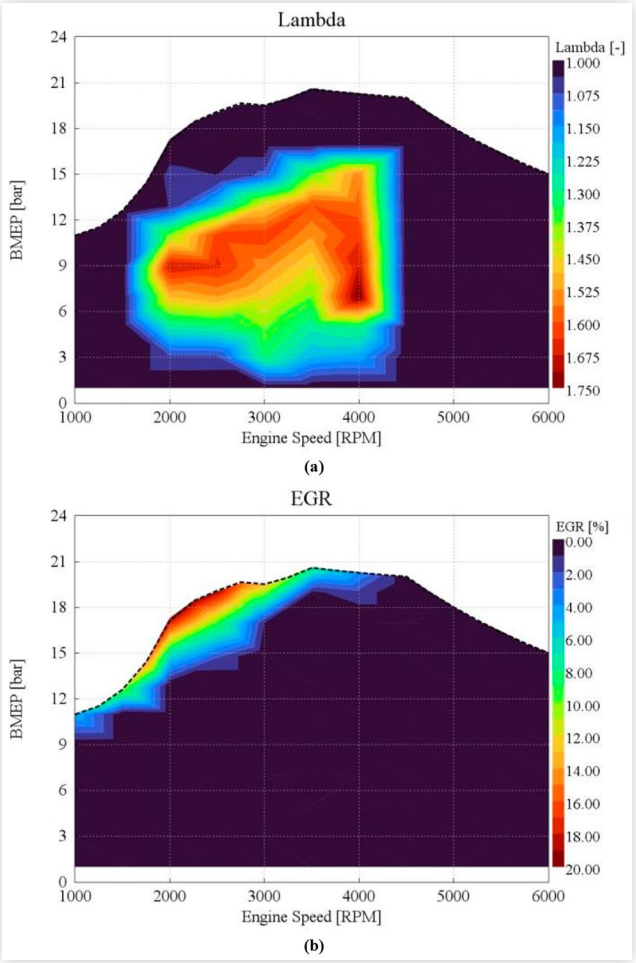

As one can see in Figure 5 (a), the PHOENICE engine is expected to operate in ultra-lean conditions for a significant portion of the engine map. Additionally, the use of Miller cycle and EGR, together with a higher turbine inlet temperature limit, should further prevent mixture enrichment for components protection at high loads. In particular, the EGR is mainly used as knock suppressor in the low-end torque region (see Figure 5 (b)).

A full-factorial DoE on electric Intake Valve Opening (eIVO) and electric Intake Valve Closing (eIVC) angles was performed to determine the best intake valves strategy capable to maximize the engine efficiency. The test matrix of the optimization is displayed in Figure 6.

It is worth to underline that the terms "electric IVO" and "electric IVC" refer to the crank angle at which the MultiAir electrohydraulic solenoid valve is actuated by the Engine Control Unit (ECU) [2], not to the actual opening angle of the intake valves. Four different eIVO values, ranging from 325 to 377.5 CA aTDCf and six eIVC levels, varying between 480 and 600 CA aTDCf were selected. Additional constraints on the minimum intake valves opening window, also referred to as lift duration, and on the maximum in-cylinder residual gas content (i.e., 22%) were also included. The latter was used as an empirical limit for the Coefficient of Variation (CoV) of the IMEP since the model does not reproduce the Cycle-to-Cycle Variability (CCV). The final optimization matrix is shown in Figure 7 (a), whereas Figure 7 (b) presents four examples of valve lifts for various eIVO and eIVC combinations at 2000 and 4000 RPM. The opening time of the electrohydraulic solenoid valve, which is independent of engine speed, causes the differences in valve lifts that can be observed for the two different engine speeds.

Optimization Results

The maps of the optimal values of eIVO and eIVC created based on DoE results were fitted and interpolated on the entire engine map as shown in Figure 8, obtaining the results reported in Figure 9.

FIGURE 7 Numerical DoE for intake valve strategy optimization. (a): Optimization matrix – (b): Example of tested valve lifts for different eIVO and eIVC combinations at 2000 and 4000 RPM.

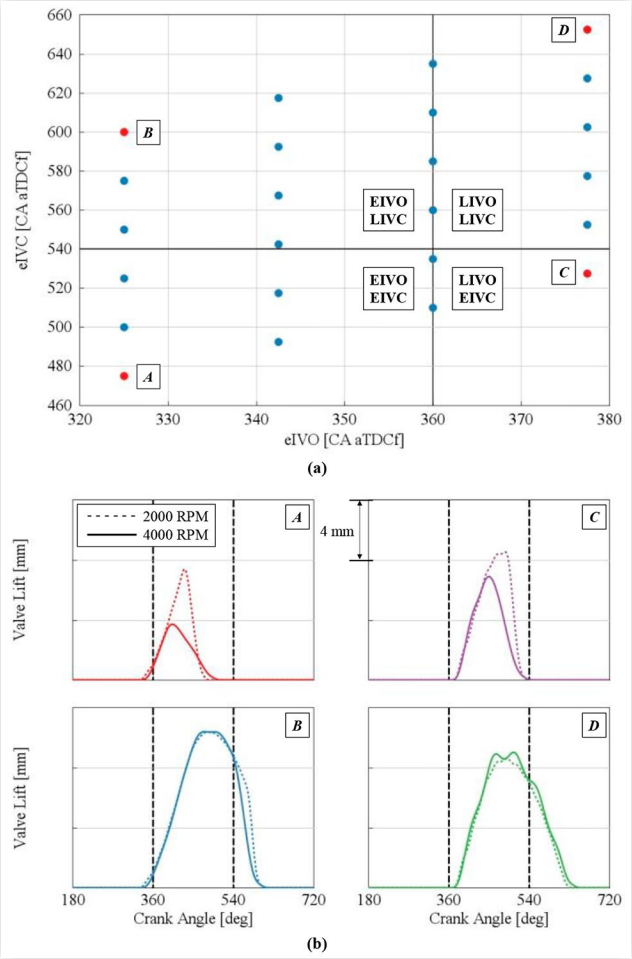

FIGURE 6 Engine operating points selected for virtual calibration.

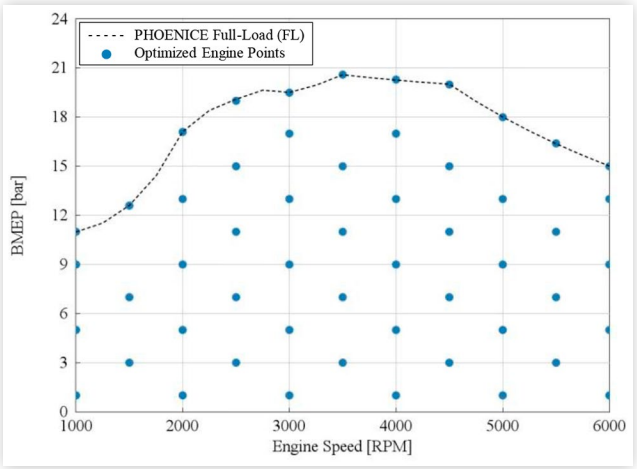

FIGURE 8 Engine operating points selected for maps generation.

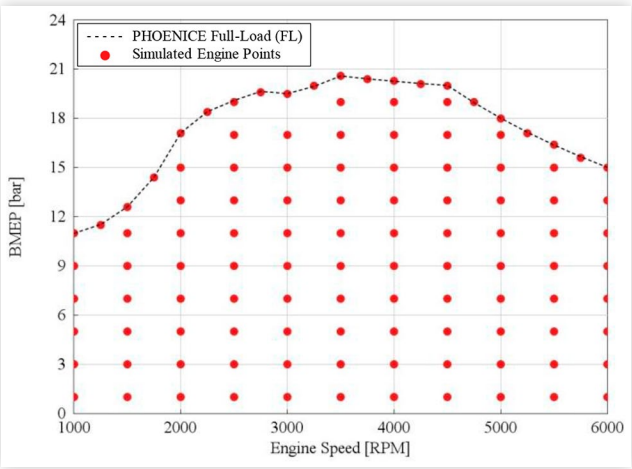

FIGURE 9 Engine steady-state virtual calibration results.

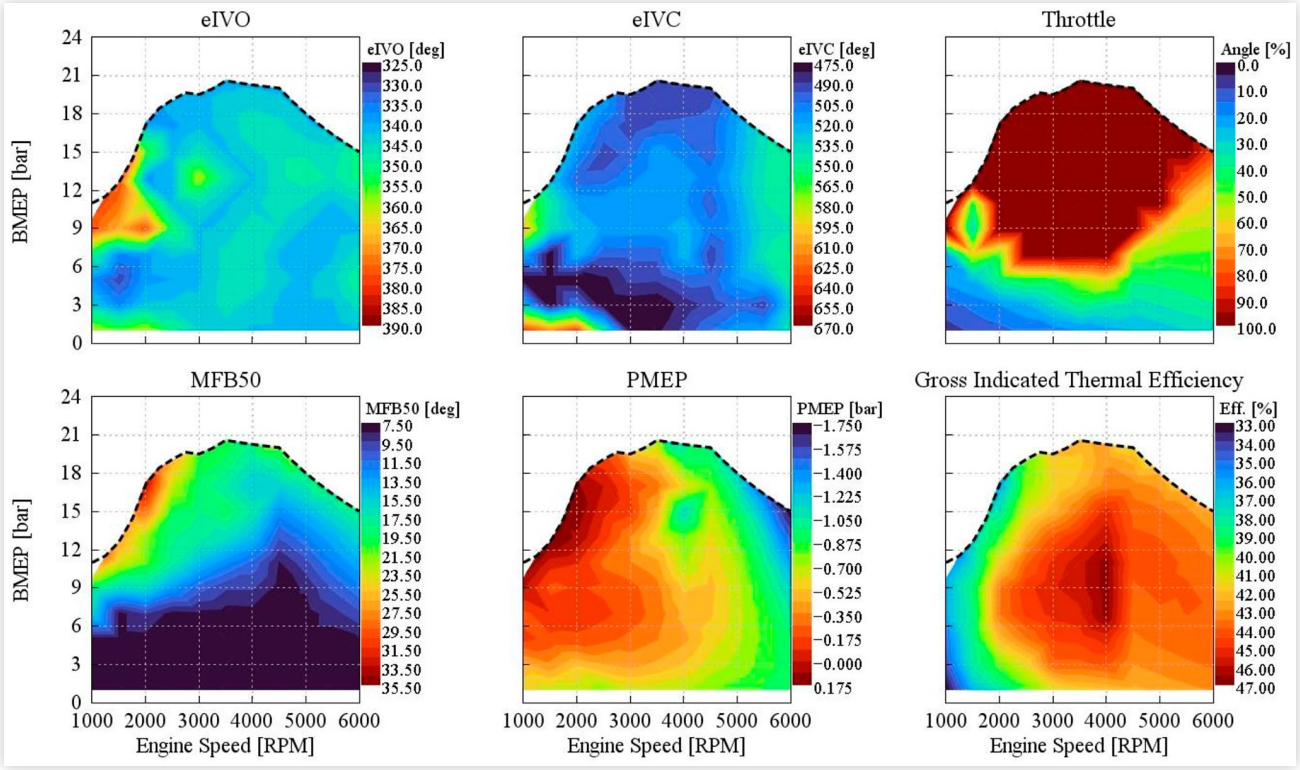

First, it is worth mentioning that the optimized intake valves strategy allows achieving a Gross Indicated Thermal Efficiency very close to the project target (i.e., 47%) at about 4000 RPM 9 bar BMEP. At low loads, the use of cycle Millerization leads to a strong reduction of the pumping losses even if with a significant worsening of the combustion as depicted in Figure 10, where the DoE results at 2000 RPM 5 bar BMEP are represented.

Moreover, despite the difference is quite small, in these operating conditions an EIVC strategy has to be preferred in comparison with a late closure. As a matter of fact, the comparison of the optimal pumping loops reported in Figure 11 highlighted a slightly higher intake pressure for the EIVC which is generated by a larger throttle opening angle and which results in a better indicated efficiency (about 0.5 efficiency points).

FIGURE 10 2000 RPM x 5 bar BMEP. DoE results.

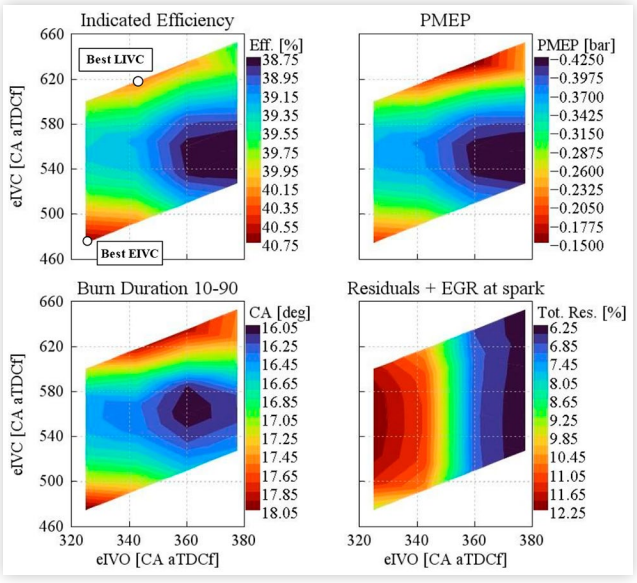

On the other hand, at high load and low speed the efficiency is mainly limited by knock, which forces the adoption of extremely retarded spark timings (see Figure 12). In this case, the use of aggressive Miller cycle, combined with the exploitation of low pressure cooled EGR, acts as a powerful tool for knock mitigation. As a matter of fact, both advanced and retarded closures allow to anticipate the center of gravity of the combustion and to reduce the residuals content since the lower boost pressure needed to reach the desired BMEP results in a wider VNT opening angle and thus lower back-pressure. Similar to the low load conditions, the performance of both EIVC and LIVC control strategies are almost equivalent also at 2500 RPM 19.1 bar BMEP, as shown in Figure 12. The former achieves a slightly better efficiency thanks to the lower residuals content which allows a small enhancement of the combustion phasing.

Conclusions

This paper described the development of a fully physical virtual test rig targeted to the support of the PHOENICE engine calibration and to the assessment of the efficiency potential of selected engine technologies.

FIGURE 11 2000 RPM x 5 bar BMEP. Comparison of pumping loops between best EIVC and best LIVC valve strategies.

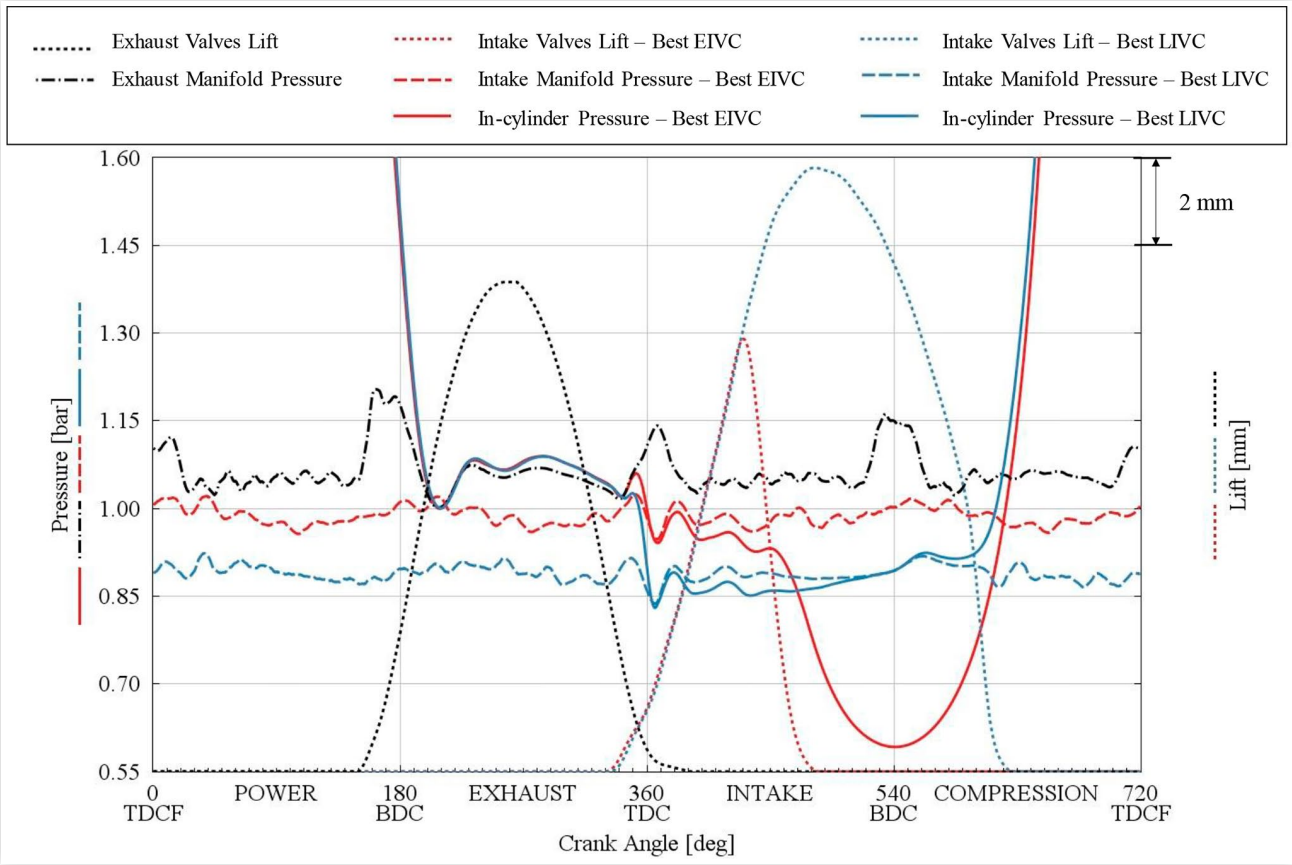

FIGURE 12 2500 RPM x 19.1 bar BMEP. DoE results.

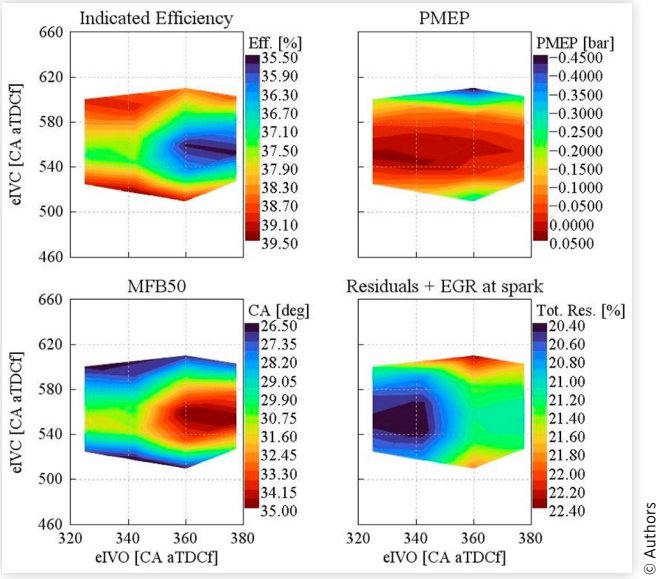

The model achieved a satisfactory correlation with preliminary experimental measurements performed on the first engine prototype at lambda = 1 without low-pressure cooled EGR. In most of the tested conditions, the main engine operating parameters showed a maximum correlation error of about 5% (Figure 5 (a)) with a good prediction of the burn rate (Figure 5(b)).

Afterwards, using the developed virtual test rig, a preliminary engine virtual calibration focused on the intake valves strategy was carried out. As a result, a maximum gross indicated efficiency of about 47% (which represents the actual target of the project) was achieved, with a wide region on the engine map in which the efficiency is higher than the 90% of its maximum value. The cycle Millerization represented a valuable solution to improve the specific fuel consumption at both low and high loads thanks to the reduction of pumping losses and knock tendency, respectively. In particular, the EIVC strategy showed a slightly higher efficiency potential with respect to LIVC even if the difference between the two was in some cases quite limited (about 0.5 efficiency points).

Future activities will focus on refining the predictive combustion model under lean and diluted engine operating conditions as well as improving the virtual engine calibration, including the optimization of both relative AFRs and EGR rates.

References

1. European Parliament Press Release, accessed March 6, 2023, https://www.europarl.europa.eu/news/en/press-

room/20230210IPR74715/fit-for-55-zero-co2-emissions-for-new-cars-and-vans-in-2035.

2. Alt, N.W., "Ready for Climate Neutrality - Demand for ICEs with Zero Carbon Footprint," in *CO2 Reduction for Transportation System Conference*, Turin, June 21-22, 2022.
3. "PHOENICE Project," accessed March 6, 2023, https://phoenice.eu/.
4. Samaras, Z., Kontses, A., Dimaratos, A., Kontses, D. et al., "A European Regulatory Perspective towards a Euro 7 Proposal," SAE Technical Paper 2022-37-0032, 2022, https://doi.org/10.4271/2022-37-0032.
5. De Marino, C., Maiorana, G., Pallotti, P., Quinto, S. et al., "The Global Small Engine 3 and 4 Cylinder Turbo: The New FCA's Family of Small High-Tech Gasoline Engines," in *39th International Vienna Motor Symposium*, Vienna, April 26-27, 2018.
6. Bernard, L., Ferrari, A., Micelli, D., Peretto, A. et al., "Electro-hydraulic Valve Control with MultiAir Technology," *MTZ Worldw* 70 (2009): 4-10, doi:https://doi.org/10.1007/BF03226988.
7. Yang, D., Lu, G., Gong, Z., Qiu, A. et al., "Development of 43% Brake Thermal Efficiency Gasoline Engine for BYD DM-i Plug-in Hybrid," SAE Technical Paper 2021-01-1241, 2021, https://doi.org/10.4271/2021-01-1241.
8. Osborne, R., Lane, A., Turner, N., Geddes, J. et al., "A New Generation Lean Gasoline Engine for Premium Vehicle CO2 Reduction," SAE Technical Paper 2021-01-0637, 2021, https://doi.org/10.4271/2021-01-0637.
9. Bunce, M., Peters, N., Pothuraju Subramanyam, S., Blaxill, H. et al., "The Impact of Advanced Fuels and Lubricants on Thermal Efficiency in a Highly Dilute Engine," *SAE Int. J. Adv. & Curr. Prac. in Mobility* 3, no. 5 (2021): 2540-2553, doi:https://doi.org/10.4271/2021-01-0462.
10. Tornatore, C., Bozza, F., de Bellis, V., Teodosio, L. et al., "Experimental and Numerical Study on the Influence of Cooled EGR on Knock Tendency, Performance and Emissions of a Downsized Spark-Ignition Engine," *Energy* 172 (2019): 968-976, doi:https://doi.org/10.1016/j.energy.2019.02.031.
11. Bourhis, G., Laget, O., Kumar, R., and Gautrot, X., "Swumble In-Cylinder Fluid Motion: a Pathway to High Efficiency Gasoline SI Engines," in *27th Aachen Colloquium Automobile and Engine Technology*, Aachen, October 8-10, 2018.
12. Gautrot, X., Bardi, M., Leroy, T., Luca, P. et al., "Swumble™ In-Cylinder Fluid Motion for High Efficiency Gasoline SI Engines: Development of the Second Generation," in *Proceedings of the SIA Powertrain and Electronics*, Rouen, November 16-29, 2020.
13. Lee, K., Bae, C., and Kang, K., "The Effects of Tumble and Swirl Flows on Flame Propagation in a Four-Valve S.I. Engine," *Applied Thermal Engineering* 27, no. 11–12 (2007): 2122-2130, doi:https://doi.org/10.1016/j.applthermaleng.2006.11.011.
14. Tahtouh, T., Millo, F., Rolando, L., Castellano, G. et al., "A Synergic Use of Innovative Technologies for the Next Generation of High Efficiency Internal Combustion Engines for PHEVs: the PHOENICE Project," SAE Technical Paper 2023-01-0224, 2023, https://doi.org/10.4271/2023-01-0224.
15. Davies, P., Bontemps, N., Tietze, T., and Faulseit, E., "Electric Turbocharging - Key Technology for Hybridized Powertrains," *MTZ Worldw* 80 (2019): 30-37, doi:https://doi.org/10.1007/s38313-019-0096-y.
16. Doornbos, G., Hemdal, S., and Dahl, D., "Reduction of Fuel Consumption and Engine-out NOx Emissions in a Lean Homogeneous GDI Combustion System, Utilizing Valve Timing and an Advanced Ignition System," SAE Technical Paper 2015-01-0776, 2015, doi:https://doi.org/10.4271/2015-01-0776.
17. Li, T., Gao, Y., Wang, J., and Chen, Z., "The Miller Cycle Effects on Improvement of Fuel Economy in a Highly Boosted, High Compression Ratio, Direct-Injection Gasoline Engine: EIVC vs. LIVC," *Energy Convers Manag* 79 (2014): 59-65, doi:https://doi.org/10.1016/j.enconman.2013.12.022.
18. Luisi, S., Doria, V., Stroppiana, A., Millo, F. et al., "Experimental Investigation on Early and Late Intake Valve Closures for Knock Mitigation through Miller Cycle in a Downsized Turbocharged Engine," SAE Technical Paper 2015-01-0760, 2015, https://doi.org/10.4271/2015-01-0760.
19. *GT-SUITE Engine Performance Application Manual, Software User Manual* (Westmont, IL, USA: Gamma Technologies, 2022)
20. Mirzaeian, M., Millo, F., and Rolando, L., "Assessment of the Predictive Capabilities of a Combustion Model for a Modern Downsized Turbocharged SI Engine," SAE Technical Paper 2016-01-0557, 2016, https://doi.org/10.4271/2016-01-0557.
21. Millo, F., Gullino, F., and Rolando, L., "Methodological Approach for 1D Simulation of Port Water Injection for Knock Mitigation in a Turbocharged DISI Engine," *Energies (Basel)* 13, no. 17 (2020), doi:https://doi.org/10.3390/en13174297.
22. Wahiduzzaman, S., Moral, T., and Sheard, S., "Comparison of Measured and Predicted Combustion Characteristics of a Four-Valve S.I. Engine," SAE Technical Paper 930613, 1993, https://doi.org/10.4271/930613.
23. Livengood, J.C. and Wu, P.C., "Correlation of Auto-ignition Phenomenon in Internal Combustion Engines and Rapid Compression Machines," in *Symposium (International) on Combustion*, vol. 5, no. 1 (Amsterdam, The Netherlands: Elsevier, 1955), 347-356.
24. By, A., Kempinski, B., and Rife, J., "Knock in Spark Ignition Engines," SAE Technical Paper 810147, 1981, doi:https://doi.org/10.4271/810147.
25. Belli, M., Danieli, G., Amelio, M., Bova, S. et al., "A Detonation Model in Spark-Ignition Engines: Preliminary Results on Engine Octane Requirement," SAE Technical Paper 841338, 1984, doi:https://doi.org/10.4271/841338.
26. Douaud, A. and Eyzat, P., "Four-Octane-Number Method for Predicting the Anti-Knock Behavior of Fuels and Engines," SAE Technical Paper 780080, 1978, doi:https://doi.org/10.4271/780080.
27. Hahn, T., "Ignition Study in Rapid Compression Machine," Bachelor's Thesis, MIT, Cambridge, MA, USA, 2006.
28. Schernus, C., Nebbia, C., Di Matteo, F., and Thewes, M., "Application of the New Kinetic Knock Model to A Downsized TGDI Engine," in *Proceedings of the Gamma Technology User Conference 2013*, Frankfurt, October 21–22, 2013.

Contact Information

Dr. Toni Tahtouh
IFP Energies Nouvelles - Mobility and Systems Division
1 et 4 avenue de Bois-Préau
92852 Rueil-Malmaison Cedex – France
toni.tahtouh@ifpen.fr

Acknowledgments

This project has received funding form the European Union's Horizon 2020 research and innovation program under Grant Agreement No. 101006841

Definitions/Abbreviations

1D-CFD - One-Dimensional Computational Fluid Dynamics
AEM - Activation Energy Multiplier
AFR - Air-to-Fuel Ratios
BMEP - Brake Mean Effective Pressure
BSFC - Brake Specific Fuel Consumption
CA aTDCf - Crank Angle after Top Dead Center of firing
CCV - Cycle-to-Cycle Variability
CoV - Coefficient of Variation
CR - Compression Ratio
CS - Charge Sustaining
CVVL - Constantly Variable Valve Lift
DDCA - Dual Dilution Combustion Approach
DISI - Direct Injection Spark Ignition
DoE - Design of Experiments
EATS - Exhaust After-Treatment System
ECU - Engine Control Unit
EGR - Exhaust Gas Recirculation
EIVC - Early Intake Valve Closing
eIVC - electric Intake Valve Closing
eIVO - electric Intake Valve Opening
GHG - Green House Gases
ICE - Internal Combustion Engine
IMEP - Indicated Mean Effective Pressure
KITM - Knock Induction Time Multiplier
KLSA - Knock-Limited Spark Advance
LIVC - Late Intake Valve Closing
NTC - Negative Temperature Coefficient
PMEP - Pumping Mean Effective Pressure
RON - Research Octane Number
RPM - Revolutions Per Minute
SCE - Single Cylinder Engine
VNT - Variable Nozzle Turbine
WG - Wastegate

Symbols

A_f - Flame Area
C_D - Dilution Effect Multiplier
C_k - Flame Kernel Development Multiplier
C_s - Turbulent Flame Speed Multiplier
C_λ - Taylor Length Multiplier
D_i - Mass Fraction of Diluents in the Unburned Zone
L_t - Turbulent Length Scale
M_b - Burned Mass
M_e - Entrained Mass
M_u - Unburned Mass
p - Pressure
R_f - Flame Radius
S_L - Laminar Flame Speed
S_T - Turbulent Flame Speed
T_u - Unburned Gas Temperature
u' - Turbulence intensity
λ - Taylor microscale
ρ_u - Unburned Gas Density
τ - Induction Time
ϕ - Equivalence Ratio

ISSN 0148-7191